Event-triggered formation control of *n*-link networked stochastic robotic manipulators

Ali Azarbahram[1] (iD)**, Naser Pariz[1], Mohammad-Bagher Naghibi-Sistani[1]
and Reihaneh Kardehi Moghaddam[2]**

Abstract

This article proposes an event-triggered control framework to satisfy the tracking formation performance for a group of uncertain non-linear *n*-link robotic manipulators. The robotic manipulators are configured as a multi-agent system and they communicate over a directed graph (digraph). Furthermore, the non-linear robotic manipulator-multi-agent systems are subject to stochastic environmental loads. By introducing extra virtual controllers in the final step of the backstepping design, a total number of *n* event-triggering mechanisms are introduced independently for each link of all the robotic manipulator agents to update the control inputs in a fully distributed manner. More precisely, the actuator of each link of a particular agent is capable of being updated independent of other link actuator updates. A rigorous proof of the convergence of all the closed-loop signals in probability is then given and the Zeno phenomenon is excluded for the control event-triggered architectures. The simulation experiments finally quantify the effectiveness of proposed approach in terms of reducing the number of control updates and handling the stochastic environmental loads.

Introduction

With the development of communication architecture, network infrastructure, and computer technology, the distributed control of multi-agent systems (MASs) has been attracted much attention in the past several years. So far, the stability analysis of linear MASs is widely studied by introducing different control frameworks (see, for instance, Li et al.[1,2]). However, the dynamics of almost all real-world systems are intrinsically non-linear including considerable uncertain terms caused by different internal or environmental forces and factors.[3] We also have to point out that some of the very important physical systems including robot manipulators (RMs), mobile robots, and spacecraft are modeled by a practical sub-class of non-linear systems called Euler–Lagrange (EL) dynamics. The trajectory tracking control of an EL system is considered in Yao[4] which guaranteed the prescribed performance subject to external disturbances, uncertainties, and actuator saturation. In Aghaei et al.,[5] a real-world application of Markov chain Monte Carlo method for Bayesian

trajectory control of an RM is studied. An adaptive neural control scheme is also studied for a single agent RM including motor dynamics in Shojaei et al.[6] to deal with model uncertainties while the prescribed performance is guaranteed.

The control of cooperative non-linear EL-MASs, however, has been a high referral topic in the fields of applied mathematics and control systems due to extensive use in real-world applications. The formation control of robot agents[7] and the consensus of multiple robots[8] are among the widely used applications of such problem formulations in the industry. The cooperative

[1]Department of Electrical Engineering, Faculty of Engineering, Ferdowsi University of Mashhad (FUM), Mashhad, Iran
[2]Department of Electrical Engineering, Islamic Azad University, Mashhad Branch, Mashhad, Iran

Corresponding author:
Naser Pariz, Department of Electrical Engineering, Faculty of Engineering, Ferdowsi University of Mashhad (FUM), Azadi Square, Razavi Khorasan Province 9177948974, Mashhad, Iran.
Email: n-pariz@um.ac.ir

performance of EL-MASs has been discussed from different points of view. Nevertheless, the shortcomings of prior methods can roughly be categorized into the following clusters (i.e. *C1–C4*):

C1: in some studied methods, each agent is supposed to access to global information regarding the Laplacian matrix of networked system. However, for a large-scale MAS, the accessibility to global information of networked system is a limiting factor. Furthermore, the relative velocity measurements between neighbor agents are usually difficult to obtain in practice; howbeit, the reported results in some precedent research papers rely explicitly on these measurements. For example, the distributed containment approaches for networked EL systems in Meng et al.[9] and Mei et al.[10] depend on the relative velocity measurements among the agents and the network Laplacian matrix.

C2: we have to note that the environmental disturbances induced by different factors certainly degrade the overall performance of real applications and in some cases give rise to instability and even system damage. As a matter of fact, environmental disturbances contain stochastic components in practice and the presence of stochastic disturbances is unavoidable in practical situations. For instance, the RM systems are often used in industrial environments, that are subject to random disturbances. The distributed control of networked EL-MASs subject to stochastic environmental loads is investigated in Shahvali and Shojaei.[11]

C3: moreover, most of the studied control architectures in the literature so far suffer from time-scheduled control frameworks. This causes high-frequency control updates and unnecessary data transmissions. In recent years, by introducing the concept of networked control systems (NCSs), the limited on-board energy resources allocated to a system have become a major concern more than ever.[12] This necessitates strategies that reduce processing such as state measurements and control input updates.[13] To reduce the number of control updates and burden of communication, the event-triggered control (ETC) scheme is introduced in recent years.[14] More understandably, data are transmitted over network or the actuators are updated only if a triggering condition is satisfied in ETC architectures. The ETC approach is also used in networked Euler–Lagrangian problem formulations.[15–17] An event-triggered (ET) robust trajectory tracking control architecture is studied for a class of uncertain EL systems in Kumari et al.[15] A fuzzy adaptive fault-tolerant ETC approach is studied in Diao et al.[16] to satisfy the finite-time tracking of single-link flexible-joint robot systems. By utilizing an ETC approach in Bu et al.,[17] the networked tracking problem is investigated for an RM subject to system uncertainties and external disturbance. However, a single RM problem formulation is considered in Kumari et al.,[15] Diao et al.,[16] and Bu et al.[17] and the cooperative performance of a networked MAS is not delved into.

The ETC approach is widely used for the consensus of linear MASs (see, for instance, Dimarogonas et al.,[14] Li et al.,[18] and Hu et al.[19]). Having analyzed the distributed ETC architectures in linear MASs, the ET scheme is also employed in investigating different applications in non-linear MASs.[20–24] In Wang et al.,[20] an ET scheme is developed for backstepping consensus of non-linear MASs in which, fuzzy state observers are introduced to estimate the unavailable information of neighbor agents. The problem of containment control is considered in Zhou et al.[21] for non-linear stochastic MASs by utilizing the backstepping approach and introducing an ET scheme. In Zhou et al.,[22] a class of non-linear MASs is considered and the problem of bipartite containment is investigated using the backstepping approach by introducing an ET rule. In Zhang et al.,[23] the containment problem is investigated by introducing ET mechanisms for a class of strict-feedback non-linear MASs. A class of non-strict-feedback MASs is also considered in Wang et al.[24] and the consensus is reached by introducing ET mechanisms and utilizing the neural networks (NNs) to approximate the unknown dynamics of agents.

So far, some research studies have addressed the ETC problem of multiple EL systems.[25–29] A discrete-time ET sliding mode framework is studied in Patel and Mehta[25] for the leader–following consensus of discrete homogeneous MASs. A distributed ETC framework is introduced for the leader–follower consensus of EL networked agents in Liu et al.[26] However, the investigated approach in Liu et al.[26] depends on the relative velocity measurements among the agents. In Yao et al.,[27] a network of EL agents is considered and the synchronization control problem is investigated by introducing ET architectures in the presence of time-varying disturbances. In Xu et al.,[28] an ETC approach is studied for the distributed tracking control of EL agents. The leaderless synchronization of EL-MASs is also investigated in Xu et al.[29] by utilizing an ET control approach. Although that time-varying external disturbances are considered and compensated in Yao et al.[27] and Xu et al.,[29] these external disturbances are assumed to be deterministic. As mentioned before, environmental disturbances contain stochastic components in practice and the deterministic control architectures such as in Yao et al.[27] and Xu et al.[29] are not applicable in the presence of stochastic disturbances and they lead to instability in most cases. In addition, the proposed ET control frameworks in Liu et al.,[26] Yao et al.,[27] and Xu et al.[28,29] depend on the global information of the network which is discussed to be a limiting factor.

We have to point out here that among the aspects of controlling the cooperative MASs, formation control of multiple agents aims at achieving and maintaining a desired configuration between the interconnected systems while trying to perform a predefined task. Here, some existing results on formation control for multiple EL systems are reviewed as follows. The formation of a

group of mobile robots is considered in Qin et al.[30] by utilizing the model predictive control approach. In Shojaei,[31] an adaptive neural proportional–integral–derivative (PID) control framework is introduced for the leader–following formation of a class of EL-MASs subject to unmodeled dynamics, uncertain parameters, and external disturbances. The ET control frameworks are also considered in investigating the formation of different forms of EL-MASs.[32–34]

C4: in considering the ET control frameworks for *n*-link RM-MASs, the actuator levels of all manipulating links are simultaneously updated in previous studies. However, this results in redundant execution of events for some particular links that are working properly in accordance with the control objectives. More understandably, since the triggering condition for the actuator updates is dependent on the norm of all the tracking errors, some manipulating links experience unnecessary updates due to inability of a few other links to show an appropriate tracking performance. Therefore, introducing an ET framework in which each manipulating link can independently update its actuator according to a triggering condition regardless of the value and update instants of other links is a topic of interest. In this case, a total number of *n* triggering thresholds are designed for each follower RM that are working independently instead of one centralized triggering rule for all the links.

Motivated by the investigated works in the existing literature, this article proposes a fully distributed ETC framework to satisfy the tracking formation of *n*-link RM-MASs. The main features of our proposed framework are listed as follows. (1) A fully distributed ET control scheme is developed for the tracking formation of RM-MASs regardless of the global information such as the eigenvalues of descriptor matrices associated with the communication network. Furthermore, the ET mechanisms are designed such that each manipulating link can independently update its actuator according to a triggering condition regardless of the value and update instants of other links. More precisely, a total number of *n* triggering thresholds are designed for each *n*-link follower RM that are working independently instead of one centralized triggering rule for all the links. (2) Since the measurement and transmission of relative velocity among any two agents is more difficult compared to the absolute velocity measurements, this article proposes a fully distributed ET framework which does not rely on the relative velocity measurements of RM-MASs. (3) The fully distributed ET control scheme is developed for RM-MASs where the differential variation of kinetics is denoted by stochastic differential equation including standard Wiener process which makes the problem formulation much more challenging and practical.

The remaining article is organized as follows. First, we introduce the preliminaries and formulate the problem. Next, the design and analysis of the fully distributed ETC problem are investigated. Then, we study the effectiveness of our proposed method by the simulation results. Finally, the final section concludes this article and provides some future directions.

Preliminaries and problem formulation

Notations

Throughout the article, matrices and vectors are denoted in the bold font and scalars by normal font. $\mathbb{R}$ is the set of real scalars; $\mathbb{R}_{\geq 0}(\mathbb{R}_{>0})$ is the set of non-negative strict positive real scalars; $\mathbb{R}^n$ is the set of real column vectors with dimension n; $|x|$ is the absolute value of $x \in \mathbb{R}$; T is the transpose of vector or square matrix; $\lambda_m(\bullet)$ and $\lambda_M(\bullet)$ are the minimum and maximum eigenvalues of their arguments, respectively.

Graph theory

Let $G := (V, E, A)$ be a directed graph (digraph) of N followers, where $V := \{v_i : i = 1, ..., N\}$ and $E := \{(v_i, v_j) \in V \times V\}$ are, respectively, the set of finite followers and the set of directed arcs, and $A := [a_{i,j}] \in \mathbb{R}_{\geq 0}^{N \times N}$ is the follower adjacency (or connectivity) matrix with element $a_{i,j} = 0$ if $(v_j, v_i) \notin E$, otherwise for $i \neq j$, $a_{i,j} \in \mathbb{R}_{>0}$. For $\forall i$, let $a_{i,i} = 0$, which implies there is no information flow from a follower to itself. The element $a_{i,j} \in \mathbb{R}_{>0}$ means that ith follower can directly access to information of jth follower. The input-degree matrix is $D := diag[d_1, ..., d_N] \in \mathbb{R}_{\geq 0}^{N \times N}$ with $d_i := \sum_{j=1}^{N} a_{i,j}$. The definition of Laplacian matrix is given by $L := D - A = [l_{i,j}] \in \mathbb{R}^{N \times N}$. A digraph is said to include a directed spanning tree if there exists a directed path from a follower (named root) to other followers. In similar way, $b_i = 0$ if the ith agent is receiving the leaders information, otherwise $b_i \in \mathbb{R}_{>0}$.

NNs

There exists a radial basis function neural network (RBFNN) for any continuous function $g(Z) : \Omega \to \mathbb{R}$ such that[35]

$$g(Z) = W^T \varphi(Z) + R(Z) \qquad (1)$$

where $W = [W_1, ..., W_r]^T \in \mathbb{R}^r$ denotes the ideal NN weight vector which minimizes approximation error $R(Z)$ over $\Omega \subset \mathbb{R}^n$. The number of NN nodes is also denoted by $r > 1$.

Furthermore, $\varphi(Z) = [\varphi_1(Z), ..., \varphi_r(Z)]^T \in \mathbb{R}^r$ denotes the activation vector of Gaussian basis functions. The approximation error is also denoted by $R(Z)$ and satisfies $|R(Z)| < \epsilon$, where ϵ is an unknown positive scalar.

The dynamics of a scalar stochastic non-linear system is described by[36]

$$dx = h(x, t)dt + \mathcal{Q}(x, t)dw \qquad (2)$$

where the state of system is $x \in \mathbb{R}$. An independent standard Wiener process of dimension r is denoted by w. Furthermore, $h : \mathbb{R} \times \mathbb{R}_{\geq 0} \to \mathbb{R}$ and $\mathcal{Q} : \mathbb{R} \times \mathbb{R}_{\geq 0} \to \mathbb{R}^{1 \times r}$ are locally Lipschitz continuous in $x \in \mathbb{R}$.

In what follows, we present the definition of pth moment semi-globally uniformly ultimately boundedness (SGUUB) of a particular stochastic system defined in equation (2).

Definition 1. For the stochastic dynamics equation (2), the system trajectory (i.e. $x(t), t \geq 0$) is pth moment SGUUB if for any initial condition $x(t_0)$ and some compact set $\Omega \subset \mathbb{R}$, there exists sufficiently small scalar $\omega > 0$ and finite-time set $T(x(t_0), \omega)$ such that $\forall t > t_0 + T$ we have[37]

$$\mathbf{E}[|x(t)|^p] < \omega$$

where $\mathbf{E}[\bullet]$ denotes the mathematical exception operator.

Remark 1. In particular, when $p = 2$, the content of Definition 1, results in SGUUB in mean square.

The following two Lemmas are used in the procedure of investigating the possible solutions of a given system described by stochastic differential equations including standard Wiener process.

Lemma 1. Let a C^2 function $\mathcal{V}(x(t))$ is defined over the stochastic system (2).[38] Then, the infinite generator of $\mathcal{V}(x(t))$ denoted by $\mathcal{L}\mathcal{V}(x(t))$ is derived as

$$\mathcal{L}\mathcal{V}(x(t)) = \frac{\partial \mathcal{V}}{\partial x} h(x, t) + \frac{1}{2} \mathrm{Tr}\left(\mathcal{Q}^{\mathrm{T}}(x, t) \frac{\partial^2 \mathcal{V}}{\partial x^2} \mathcal{Q}(x, t) \right) \qquad (3)$$

Lemma 2. Suppose that a C^2 function $\mathcal{V}(x(t)) : \mathbb{R} \to \mathbb{R}_{\geq 0}$ is defined. If there exist class K_∞ functions $\varsigma_1(\bullet)$ and $\varsigma_2(\bullet)$, two positive constants c_1 and c_2 such that $\forall x(t) \in \mathbb{R}$ and $\forall t \geq t_0 \geq 0$, we have[39]

$$\begin{cases} \varsigma_1(|x(t)|) \leq \mathcal{V}(x(t)) \leq \varsigma_2(|x(t)|) \\ \mathcal{L}\mathcal{V}(x(t)) \leq -c_1 \mathcal{V}(x(t)) + c_2 \end{cases} \qquad (4)$$

then there exists a unique strong solution of the system (2) for each $x(t_0) \in \mathbb{R}$ which satisfies

$$\mathbf{E}[\mathcal{V}(x(t))] \leq e^{-c_1(t-t_0)} \mathcal{V}(x(t_0)) + \frac{c_2}{c_1} \qquad (5)$$

The following Lemma is also of much importance in the stability analysis of different classes of non-linear systems.

Lemma 3 (Young's inequality). For any vector set $(\mathbf{s}_1, \mathbf{s}_2) \in \mathbb{R}^n$, the following inequality holds[37]

$$\mathbf{s}_1^{\mathrm{T}} \mathbf{s}_2 \leq \frac{\varepsilon^c}{c} \|\mathbf{s}_1\|^c + \frac{1}{d\varepsilon^d} \|\mathbf{s}_2\|^d$$

where $\varepsilon > 0, c > 1, d > 1$, and $(c-1)(d-1) = 1$.

Property 1. For any real positive constant ϖ_1 and real number ϖ_2, the following inequality holds true

$$|\varpi_2| < \frac{\varpi_2^2}{\sqrt{\varpi_2^2 + \varpi_1^2}} + \varpi_1$$

Problem definition

A networked group of n-link RMs is supposed to follow a desired trajectory while trying to maintain a predetermined formation among themselves. Let $\boldsymbol{q}_{i,1} = [q_{i,1}^{[1]}, q_{i,1}^{[2]}, \ldots, q_{i,1}^{[n]}]^{\mathrm{T}} \in \mathbb{R}^n$ and $\boldsymbol{q}_{i,2} = [q_{i,2}^{[1]}, q_{i,2}^{[2]}, \ldots, q_{i,2}^{[n]}]^{\mathrm{T}} \in \mathbb{R}^n$ denote, respectively, the joint position and velocity vectors for ith RM, $\forall i = 1, ..., N$ with respect to the ιth link of each manipulator. Then, the dynamics of each RM follower agent is described by the following stochastic differential equations

$$\begin{cases} d\boldsymbol{q}_{i,1} = \boldsymbol{q}_{i,2}dt \\ d\boldsymbol{q}_{i,2} = \mathcal{M}_i^{-1}[-C_i(\boldsymbol{q}_{i,1}, \boldsymbol{q}_{i,2})\boldsymbol{q}_{i,2} - \boldsymbol{D}_i(\boldsymbol{q}_{i,1})\boldsymbol{q}_{i,2} \\ \qquad\quad -\boldsymbol{G}_i(\boldsymbol{q}_{i,1}) + \boldsymbol{u}_i]dt + \mathcal{G}_i(\boldsymbol{q}_{i,2}, t)dw \end{cases} \qquad (6)$$

where $\boldsymbol{u}_i = [u_i^{[1]}, u_i^{[2]}, \ldots, u_i^{[n]}]^{\mathrm{T}} \in \mathbb{R}^n$ denotes the input torque. The exogenous environmental disturbances vector is expressed by w which is an independent standard Wiener process of dimension r. In addition, $\mathcal{G}_i(\boldsymbol{q}_{i,2}, t) : \mathbb{R}^n \times \mathbb{R}_{\geq 0} \to \mathbb{R}^{n \times r}$ is an unknown locally Lipschitz function in $\boldsymbol{q}_{i,2}$.

Property 2. The inertia matrix $\mathcal{M}_i$ is always symmetric positive-definite with the following properties

$$\begin{cases} \mathcal{M}_i = \mathcal{M}_i^{\mathrm{T}} > 0 \\ \min(\lambda_{\mathrm{m}}\{\mathcal{M}_i\})\|\boldsymbol{h}\|^2 \leq \boldsymbol{h}^{\mathrm{T}}\mathcal{M}_i\boldsymbol{h} \leq \max(\lambda_{\mathrm{M}}\{\mathcal{M}_i\})\|\boldsymbol{h}\|^2 \\ \forall \boldsymbol{h} \in \mathbb{R}^n \\ \min(\lambda_{\mathrm{m}}\{\mathcal{M}_i\}) \leq \max(\lambda_{\mathrm{M}}\{\mathcal{M}_i\}) < \infty \end{cases}$$

The total Coriolis and centripetal acceleration matrix is denoted by $C_i(\boldsymbol{q}_{i,1}, \boldsymbol{q}_{i,2})$, and moreover, the damping matrix is $\boldsymbol{D}_i(\boldsymbol{q}_{i,1})$. Furthermore, $\boldsymbol{G}_i(\boldsymbol{q}_{i,1})$ is the vector of the gravity effects.

Property 3. The following features are preserved for the total Coriolis and centripetal acceleration and the damping matrices

$$
\begin{cases}
\boldsymbol{C}_i = -\boldsymbol{C}_i^{\mathrm{T}}, \boldsymbol{D}_i = \boldsymbol{D}_i^{\mathrm{T}} > 0 \\
\boldsymbol{h}^{\mathrm{T}}(\dot{\boldsymbol{\mathcal{M}}}_i - 2\boldsymbol{C}_i)\boldsymbol{h} = 0, \forall \boldsymbol{h} \in \mathbb{R}^n \\
\min(\lambda_{\mathrm{m}}\{\boldsymbol{D}_i\})\|\boldsymbol{h}\|^2 \leqslant \boldsymbol{h}^{\mathrm{T}}\boldsymbol{D}_i\boldsymbol{h} \leqslant \max(\lambda_{\mathrm{M}}\{\boldsymbol{D}_i\})\|\boldsymbol{h}\|^2 \\
\forall \boldsymbol{h} \in \mathbb{R}^n \\
\min(\lambda_{\mathrm{m}}\{\boldsymbol{D}_i\}) \leqslant \max(\lambda_{\mathrm{M}}\{\boldsymbol{D}_i\}) < \infty
\end{cases}
$$

Property 4. For the gravity effect vector, one has $\|\boldsymbol{G}_i(\boldsymbol{q}_{i,1})\| \leqslant \gamma_g$, where γ_g is an unknown positive constant.

In what follows, the content of Definition 1 is generalized to obtain cooperatively semi-globally uniformly ultimately boundedness (CSGUUB) of closed-loop system (6) when the RM team is supposed to maintain a desired formation among themselves.

Definition 2. Suppose that for the ith agent, the predetermined desired formation position with respect to the leader is denoted by $\bar{\boldsymbol{\eta}}_i \in \mathbb{R}^n$, where $\bar{\boldsymbol{\eta}}_i = [\bar{\eta}_i^{[1]}, \bar{\eta}_i^{[2]}, \ldots, \bar{\eta}_i^{[n]}]^{\mathrm{T}}$. In addition, consider that $\boldsymbol{q}_{r,1} = [q_{r,1}^{[1]}, q_{r,1}^{[2]}, \ldots, q_{r,1}^{[n]}]^{\mathrm{T}} \in \mathbb{R}^n$ is the reference trajectory to be followed by the RMs. Then, under the control protocol $\boldsymbol{u}_i(t)$, a group of stochastic RMs equation (6) is said pth moment CSGUUB while maintained the predefined formation among the agents, if for any initial states $\boldsymbol{q}_{i,1}(t_0) \in \mathbb{R}^n$ and $\boldsymbol{q}_{i,2}(t_0) \in \mathbb{R}^n$, there exists sufficiently small scalar $\omega > 0$ and finite-time set $T_i(\boldsymbol{q}_{i,1}(t_0), \boldsymbol{q}_{i,2}(t_0), \omega)$ such that

$$
\mathbf{E}\left[\left|q_{i,1}^{[\iota]}(t) - \bar{\eta}_i^{[\iota]}(t) - q_{r,1}^{[\iota]}(t)\right|^p\right] < \omega, \forall t > t_0 + T_i \quad (7)
$$

for all $\iota = 1, \ldots, n$ and $i = 1, 2, \ldots, N$.

Remark 2. The RM systems are often used in industrial environments that are subject to random disturbances. Actually, the environmental stochastic disturbances induced by different factors certainly degrade the overall performance of real applications and in some cases give rise to instability and even system damage. If dw/dt is bounded, the problem is formulated as deterministic control of RMs. In deterministic problems, $\sup_{t \geqslant 0} \|dw/dt\|$ is well-defined. However, as mentioned before, the environmental disturbances contain in fact stochastic components. In this case, is unbounded and $w(t)$ is considered as a standard Wiener process. The deterministic control architectures are not applicable in stochastic cases and they lead to instability in most cases.

Assumption 1. The desired reference trajectory and the predetermined formation position with respect to the leader are bounded, deterministic and they also satisfy $q_{r,1}^{[\iota]}(t) \in C^2$ and $\bar{\eta}_i^{[\iota]}(t) \in C^2$.

Design and analysis

We now define the formation error vector $\boldsymbol{\zeta}_{i,1}$ as $\boldsymbol{\zeta}_{i,1} = [\zeta_{i,1}^{[1]}, \zeta_{i,1}^{[2]}, \ldots, \zeta_{i,1}^{[n]}]^{\mathrm{T}}$. The ιth element of ith RM formation error (i.e. $\zeta_{i,1}^{[\iota]}$) is then written as

$$
\begin{aligned}
\zeta_{i,1}^{[\iota]} = &\sum_{j \in N_i} a_{i,j}\left(q_{i,1}^{[\iota]}(t) - q_{j,1}^{[\iota]}(t) - \eta_{i,j}^{[\iota]}(t)\right) \\
&+ b_i\left(q_{i,1}^{[\iota]}(t) - q_{r,1}^{[\iota]}(t) - \bar{\eta}_i^{[\iota]}(t)\right)
\end{aligned} \quad (8)
$$

where, $\eta_{i,j}^{[\iota]}(t) = \bar{\eta}_i^{[\iota]}(t) - \bar{\eta}_j^{[\iota]}(t) \in \mathbb{R}$, for $i = 1, \ldots, N$ and $\iota = 1, \ldots, n$.

The following stochastic differential equation is then derived

$$
\begin{aligned}
\mathrm{d}\zeta_{i,1}^{[\iota]} = &\left[\sum_{j \in N_i} a_{i,j}\left(q_{i,2}^{[\iota]}(t) - q_{j,2}^{[\iota]}(t) - \dot{\eta}_{i,j}^{[\iota]}(t)\right)\right. \\
&\left.+ b_i\left(q_{i,2}^{[\iota]}(t) - \dot{q}_{r,1}^{[\iota]}(t) - \dot{\bar{\eta}}_i^{[\iota]}(t)\right)\right]\mathrm{d}t
\end{aligned} \quad (9)
$$

Furthermore, the second surface of error is defined as

$$
\boldsymbol{\zeta}_{i,2} = \boldsymbol{q}_{i,2} - \boldsymbol{\alpha}_{i,1}
$$

where $\boldsymbol{\zeta}_{i,2} = [\zeta_{i,2}^{[1]}, \zeta_{i,2}^{[2]}, \ldots, \zeta_{i,2}^{[n]}]^{\mathrm{T}}$. In addition, $\boldsymbol{\alpha}_{i,1} = [\alpha_{i,1}^{[1]}, \alpha_{i,1}^{[2]}, \ldots, \alpha_{i,1}^{[n]}]^{\mathrm{T}}$ is a virtual control vector to be designed. The ιth element of the second surface of error for the ith RM is then derived as

$$
\zeta_{i,2}^{[\iota]} = q_{i,2}^{[\iota]} - \alpha_{i,1}^{[\iota]} \quad (10)
$$

Now, a Lyapunov function candidate is constructed as

$$
\mathcal{V}_{i,1} = \frac{1}{2}\sum_{\iota=1}^n \zeta_{i,1}^{[\iota]2} \quad (11)
$$

From graph theory, we know that the input-degree matrix is denoted by $D := diag[d_1, \ldots, d_N] \in \mathbb{R}_{\geqslant 0}^{N \times N}$ with $d_i := \sum_{j=1}^N a_{i,j}$. Then, by taking into account the second layer error in equation (10), and according to equation (3), the Lyapunov function candidate equation (11) results in the following infinite generator

$$\mathcal{L}\mathcal{V}_{i,1} = \sum_{\iota=1}^{n} \zeta_{i,1}^{[\iota]} \left[(d_i + b_i)\left(\zeta_{i,2}^{[\iota]} + \alpha_{i,1}^{[\iota]} \right) - b_i \dot{q}_{r,1}^{[\iota]} \right.$$
$$\left. - d_i \dot{\eta}_{i,j}^{[\iota]}(t) - b_i \dot{\bar{\eta}}_i^{[\iota]}(t) - \sum_{j \in N_i} a_{i,j}\left(q_{j,2}^{[\iota]}(t) \right) \right] \tag{12}$$

The virtual control is now designed as

$$\alpha_{i,1}^{[\iota]}(t) = \frac{1}{(d_i + b_i)} \left[-K_{i,1}^{[\iota]} \zeta_{i,1}^{[\iota]} + b_i \dot{q}_{r,1}^{[\iota]} + d_i \dot{\eta}_{i,j}^{[\iota]}(t) \right.$$
$$\left. + b_i \dot{\bar{\eta}}_i^{[\iota]}(t) + \sum_{j \in N_i} a_{i,j}\left(q_{j,2}^{[\iota]}(t) \right) \right] \tag{13}$$

where $K_{i,1}^{[\iota]}$ for $i = 1, \ldots, N$ and $\iota = 1, \ldots, n$ is a control gain constant to be chosen appropriately.

The kinetics in equation (6) can be rewritten as

$$\mathrm{d}q_{i,2} = \left[g_{i,1}\left(q_{i,1}, q_{i,2} \right) - \bar{G}\left(q_{i,1} \right) + \bar{u}_i \right] \mathrm{d}t + \mathcal{G}_i\left(q_{i,2}, t \right) \mathrm{d}w \tag{14}$$

where

$$g_{i,1}(.) = \mathcal{M}_i^{-1}\left(-C_i\left(q_{i,1}, q_{i,2} \right) q_{i,2} - D_i\left(q_{i,1} \right) q_{i,2} \right)$$

Furthermore

$$\bar{G}_i\left(q_{i,1} \right) = \mathcal{M}_i^{-1} G_i\left(q_{i,1} \right)$$

and $\bar{u}_i = \mathcal{M}_i^{-1} u_i$ with $\bar{u}_i = [\bar{u}^{[1]}, \bar{u}^{[2]}, \ldots, \bar{u}^{[n]}]^{\mathrm{T}}$.

In addition, $\bar{G}_i\left(q_{i,1} \right) = [\bar{G}_i^{[1]}, \bar{G}_i^{[2]}, \ldots, \bar{G}_i^{[n]}]^{\mathrm{T}}$ and $g_{i,1}(.) = [g_{i,1}^{[1]}, g_{i,1}^{[2]}, \ldots, g_{i,1}^{[n]}]^{\mathrm{T}}$.

We expand the Lyapunov function candidate to have

$$\mathcal{V}_{i,2} = \mathcal{V}_{i,1} + \frac{1}{4} \sum_{\iota=1}^{n} \zeta_{i,2}^{[\iota]4}. \tag{15}$$

Denote the ιth row of $\mathcal{G}_i$ by $\mathcal{G}_{i,\iota}^{\mathrm{T}}$. From Lemma 3, one deduces that

$$(d_i + b_i) \sum_{\iota=1}^{n} \zeta_{i,1}^{[\iota]} \zeta_{i,2}^{[\iota]} \leqslant \frac{d_i + b_i}{2} \left(\sum_{\iota=1}^{n} \zeta_{i,1}^{[\iota]2} + \sum_{\iota=1}^{n} \zeta_{i,2}^{[\iota]2} \right)$$

Now, by taking equations (13) and (14), and the aforementioned statements into account, the following holds true by applying Lemma 1

$$\mathcal{L}\mathcal{V}_{i,2} \leqslant - \sum_{\iota=1}^{n} \left[K_{i,1}^{[\iota]} - \frac{d_i + b_i}{2} \right] \zeta_{i,1}^{[\iota]2} + \frac{d_i + b_i}{2} \sum_{\iota=1}^{n} \zeta_{i,2}^{[\iota]2}$$
$$+ \sum_{\iota=1}^{n} \zeta_{i,2}^{[\iota]3} \left[g_{i,1}^{[\iota]} - \bar{G}_i^{[\iota]} + \bar{u}_i^{[\iota]} - \mathcal{L}\alpha_{i,1}^{[\iota]} \right]$$
$$+ \frac{3}{2} \sum_{\iota=1}^{n} \zeta_{i,2}^{[\iota]2} \left\| \mathcal{G}_{i,\iota}^{\mathrm{T}} \right\|^2 \tag{16}$$

Define an unknown function of the form

$$g_{i,2}^{[\iota]}(.) = g_{i,1}^{[\iota]} - \mathcal{L}\alpha_{i,1}^{[\iota]} \tag{17}$$

The NNs' approach is utilized to approximate $g_{i,2}^{[\iota]}(.)$ such that for positive constants $\epsilon_i^{[\iota]}$, one has

$$g_{i,2}^{[\iota]}(.) = \boldsymbol{U}_{i,\iota}^{\mathrm{T}} \boldsymbol{\varphi}_{i,\iota} + \epsilon_i^{[\iota]} \tag{18}$$

where $\boldsymbol{U}_{i,\iota} \in \mathbb{R}^n$ is an unknown vector and $\boldsymbol{\varphi}_{i,\iota}$ is the activation vector of Gaussian basis functions. Based on Young's inequality, one obtains

$$\frac{3}{2} \sum_{\iota=1}^{n} \zeta_{i,2}^{[\iota]2} \left\| \mathcal{G}_{i,\iota}^{\mathrm{T}} \right\|^2 \leqslant \frac{3}{4} \left[\sum_{\iota=1}^{n} \varepsilon_i^2 \zeta_{i,2}^{[\iota]4} \left\| \mathcal{G}_{i,\iota}^{\mathrm{T}} \right\|^4 + \frac{n}{\varepsilon_i^2} \right] \tag{19}$$

and

$$\frac{d_i + b_i}{2} \sum_{\iota=1}^{n} \zeta_{i,2}^{[\iota]2} \leqslant \frac{d_i + b_i}{4} \left[\sum_{\iota=1}^{n} \varepsilon_i^2 \zeta_{i,2}^{[\iota]4} + \frac{n}{\varepsilon_i^2} \right] \tag{20}$$

where ε_i for $i = 1, \ldots, N$ is a strictly positive design constant defined in Lemma 3.

Another set of unknown functions are also defined as

$$Q_i^{[\iota]} = \epsilon_i^{[\iota]} - \bar{G}_i^{[\iota]} + \frac{3}{4} \varepsilon_i^2 \zeta_{i,2}^{[\iota]} \left\| \mathcal{G}_{i,\iota}^{\mathrm{T}} \right\|^4$$

for all $i = 1, \ldots, N$ and $\iota = 1, \ldots, n$. Then, one has

$$\mathcal{L}\mathcal{V}_{i,2} \leqslant - \sum_{\iota=1}^{n} \left[K_{i,1}^{[\iota]} - \frac{d_i + b_i}{2} \right] \zeta_{i,1}^{[\iota]2} + \frac{d_i + b_i}{4} \sum_{\iota=1}^{n} \varepsilon_i^2 \zeta_{i,2}^{[\iota]4}$$
$$+ \sum_{\iota=1}^{n} \zeta_{i,2}^{[\iota]3} \left[\boldsymbol{U}_{i,\iota}^{\mathrm{T}} \boldsymbol{\varphi}_{i,\iota} + Q_i^{[\iota]} + \bar{u}_i^{[\iota]} \right]$$
$$+ \frac{n}{4\varepsilon_i^2}(3 + d_i + b_i) \tag{21}$$

We have to note that $\sum_{\iota=1}^{n} \zeta_{i,2}^{[\iota]} \boldsymbol{U}_{i,\iota}^{\mathrm{T}} \boldsymbol{\varphi}_{i,\iota}$ is less than or equal to $\sum_{\iota=1}^{n} |\zeta_{i,2}^{[\iota]}| \, \| \boldsymbol{U}_{i,\iota}^{\mathrm{T}} \| \| \boldsymbol{\varphi}_{i,\iota} \|$.

According to Property 1, for any two real-positive constants $\varpi_{i,1}$ and $\varpi_{i,2}$, the following inequalities hold true

$$\sum_{\iota=1}^{n} \left| \zeta_{i,2}^{[\iota]} \right| \left\| \boldsymbol{\varphi}_{i,\iota} \right\| \leqslant \sum_{\iota=1}^{n} \frac{\zeta_{i,2}^{[\iota]2} \left\| \boldsymbol{\varphi}_{i,\iota} \right\|^2}{\sqrt{\zeta_{i,2}^{[\iota]2} \left\| \boldsymbol{\varphi}_{i,\iota} \right\|^2 + \varpi_{i,1}^2}} + n\varpi_{i,1}$$

$$\sum_{\iota=1}^{n} \left| \zeta_{i,2}^{[\iota]} \right| \leqslant \sum_{\iota=1}^{n} \frac{\zeta_{i,2}^{[\iota]2}}{\sqrt{\zeta_{i,2}^{[\iota]2} + \varpi_{i,2}^2}} + n\varpi_{i,2}$$

Denote the positive constants $\| \boldsymbol{U}_{i,\iota}^{\mathrm{T}} \|$ and $|Q_i^{[\iota]}|$ with $\mu_{i,1}^{[\iota]}$ and $\mu_{i,2}^{[\iota]}$, respectively. Then, for $i = 1, \ldots, N$ and $\iota = 1, \ldots, n$, the approximation errors are defined as $\tilde{\mu}_{i,1}^{[\iota]} = \mu_{i,1}^{[\iota]} - \hat{\mu}_{i,1}^{[\iota]}$ and $\tilde{\mu}_{i,2}^{[\iota]} = \mu_{i,2}^{[\iota]} - \hat{\mu}_{i,2}^{[\iota]}$.

Now, expand again the Lyapunov function candidate to have

$$\mathcal{V}_{i,3} = \mathcal{V}_{i,2} + \sum_{\iota=1}^{n} \frac{1}{2\gamma_{i,1}^{[\iota]}} \tilde{\mu}_{i,1}^{[\iota]2} + \sum_{\iota=1}^{n} \frac{1}{2\gamma_{i,2}^{[\iota]}} \tilde{\mu}_{i,2}^{[\iota]2} \tag{22}$$

with positive constants $\gamma_{i,1}^{[\iota]}$ and $\gamma_{i,2}^{[\iota]}$, for $i = 1, \ldots, N$ and $\iota = 1, \ldots, n$. This results in

$$\begin{aligned}
\mathcal{L}\mathcal{V}_{i,3} \leqslant &-\sum_{\iota=1}^{n} \left[K_{i,1}^{[\iota]} - \frac{d_i + b_i}{2} \right] \zeta_{i,1}^{[\iota]2} + \frac{d_i + b_i}{4} \sum_{\iota=1}^{n} \varepsilon_i^2 \zeta_{i,2}^{[\iota]4} \\
&+ \sum_{\iota=1}^{n} \zeta_{i,2}^{[\iota]3} \left[\bar{u}_i^{[\iota]} + \frac{\zeta_{i,2}^{[\iota]} \left\| \boldsymbol{\varphi}_{i,\iota} \right\|^2}{\sqrt{\zeta_{i,2}^{[\iota]2} \left\| \boldsymbol{\varphi}_{i,\iota} \right\|^2 + \varpi_{i,1}^2}} \mu_{i,1}^{[\iota]} \right. \\
&+ \left. \frac{\zeta_{i,2}^{[\iota]}}{\sqrt{\zeta_{i,2}^{[\iota]2} + \varpi_{i,2}^2}} \mu_{i,2}^{[\iota]} \right] \\
&- \sum_{\iota=1}^{n} \frac{1}{\gamma_{i,1}^{[\iota]}} \tilde{\mu}_{i,1}^{[\iota]} \dot{\hat{\mu}}_{i,1}^{[\iota]} - \sum_{\iota=1}^{n} \frac{1}{\gamma_{i,2}^{[\iota]}} \tilde{\mu}_{i,2}^{[\iota]} \dot{\hat{\mu}}_{i,2}^{[\iota]} + \mathcal{F}_i
\end{aligned} \tag{23}$$

where

$$\mathcal{F}_i = n(\varpi_{i,1} + \varpi_{i,2}) + \frac{n}{4\varepsilon_i^2}(3 + d_i + b_i) \tag{24}$$

Now, the adaptive laws are proposed as

$$\dot{\hat{\mu}}_{i,1}^{[\iota]} = \gamma_{i,1}^{[\iota]} \left(\frac{\zeta_{i,2}^{[\iota]4} \left\| \boldsymbol{\varphi}_{i,\iota} \right\|^2}{\sqrt{\zeta_{i,2}^{[\iota]2} \left\| \boldsymbol{\varphi}_{i,\iota} \right\|^2 + \varpi_{i,1}^2}} - \sigma_{i,1}^{[\iota]} \hat{\mu}_{i,1}^{[\iota]} \right) \tag{25}$$

$$\dot{\hat{\mu}}_{i,2}^{[\iota]} = \gamma_{i,2}^{[\iota]} \left(\frac{\zeta_{i,2}^{[\iota]4}}{\sqrt{\zeta_{i,2}^{[\iota]2} + \varpi_{i,2}^2}} - \sigma_{i,2}^{[\iota]} \hat{\mu}_{i,2}^{[\iota]} \right) \tag{26}$$

with σ-modification parameters $\sigma_{i,1}^{[\iota]}$ and $\sigma_{i,2}^{[\iota]}$ for all $i = 1, \ldots, N$ and $\iota = 1, \ldots, n$.

Distributed ET controller design

Let $t_{i,0}^{[\iota]}, t_{i,1}^{[\iota]}, \ldots, t_{i,\kappa}^{[\iota]}, t_{i,\kappa+1}^{[\iota]}, \ldots$ denote the time sequence at which the actuator events are detected for the ιth element of the control input vector (i.e. $\bar{u}_i^{[\iota]}$) and the actuator information is updated. In this case, the first control update instant of each element is set to $t_{i,0}^{[\iota]} = 0$. Having triggered the most recent event at $t_{i,\kappa}^{[\iota]}$, then the next event is triggered at $t_{i,\kappa+1}^{[\iota]}$ which satisfies the following ET condition

$$t_{i,\kappa+1}^{[\iota]} = \inf\left\{ t \,|\, t > t_{i,\kappa}^{[\iota]}, \left| \Delta_i^{[\iota]} \right| - \mathcal{E}_i^{[\iota]} \geqslant 0 \right\} \tag{27}$$

where $\mathcal{E}_i^{[\iota]}(t) = v_{i,1}^{[\iota]} + v_{i,2}^{[\iota]}(t)$. Furthermore, $v_{i,1}^{[\iota]}$ is a positive design constant and $\int_0^t v_{i,2}^{[\iota]}(\tau)d\tau < \infty$. For the time interval between two consecutive event instants, the measurement errors are denoted by $\Delta_i^{[\iota]}(t) = \bar{u}_i^{[\iota]}(t) - \alpha_{i,2}^{[\iota]}(t)$. Moreover, $\forall t \in [t_{i,\kappa}^{[\iota]}, t_{i,\kappa+1}^{[\iota]})$, one has $\bar{u}_i^{[\iota]}(t) = \alpha_{i,2}^{[\iota]}(t_{i,\kappa}^{[\iota]})$. In addition, $\alpha_{i,2}^{[\iota]}$ is a virtual control law as

$$\begin{aligned}
\alpha_{i,2}^{[\iota]} = &-K_{i,2}^{[\iota]} \zeta_{i,2}^{[\iota]} - \frac{\zeta_{i,2}^{[\iota]} \left\| \boldsymbol{\varphi}_{i,1} \right\|^2}{\sqrt{\zeta_{i,2}^{[\iota]2} \left\| \boldsymbol{\varphi}_{i,\iota} \right\|^2 + \varpi_{i,1}^2}} \hat{\mu}_{i,1}^{[\iota]} \\
&- \frac{\zeta_{i,2}^{[\iota]}}{\sqrt{\zeta_{i,2}^{[\iota]2} + \varpi_{i,2}^2}} \hat{\mu}_{i,2}^{[\iota]}
\end{aligned} \tag{28}$$

where $K_{i,2}^{[\iota]}$ for $i = 1, \ldots, N$ and $\iota = 1, \ldots, n$ is a control gain constant.

Remark 3. The function $v_{i,2}^{[\iota]}(t)$ for $\iota = 1, \ldots, n$ is chosen as a decaying exponential function (such as $v_{i,2}^{[\iota]}(t) = a\exp(-t/\tau)$ for a constant a and time constant τ). These terms add an acceptable margin to the triggering threshold $\mathcal{E}_i^{[\iota]}(t)$ at the beginning moments of system performance when the initial formation errors are relatively large in absolute value. This prevents over-triggering at the beginning moments. The effect of function $v_{i,2}^{[\iota]}(t)$ for $i = 1, \ldots, N$ and $\iota = 1, \ldots, n$ on the triggering condition vanishes almost after a certain period of time. Since then, the positive design constant $v_{i,1}^{[\iota]}$ is in charge of deciding on triggering moments.

By adding and subtracting $\alpha_{i,2}^{[\iota]}$ to $\dot{\zeta}_{i,2}^{[\iota]}$, and taking equations (25), (26), and (28) into account, the infinite generator in equation (23) results in

$$\mathcal{L}\mathcal{V}_{i,3} \leqslant$$

$$-\sum_{\iota=1}^{n}\left[K_{i,1}^{[\iota]} - \frac{d_i + b_i}{2}\right]\varsigma_{i,1}^{[\iota]2} - \sum_{\iota=1}^{n}\left[K_{i,2}^{[\iota]} - \frac{(d_i + b_i)\varepsilon_i^2}{4}\right]\varsigma_{i,2}^{[\iota]4}$$

$$-\sum_{\iota=1}^{n}\frac{1}{2}\sigma_{i,1}^{[\iota]}\tilde{\mu}_{i,1}^{[\iota]2} - \sum_{\iota=1}^{n}\frac{1}{2}\sigma_{i,2}^{[\iota]}\tilde{\mu}_{i,2}^{[\iota]2} + \sum_{\iota=1}^{n}\frac{1}{2}\sigma_{i,1}^{[\iota]}\mu_1^{[\iota]2}$$

$$+\sum_{\iota=1}^{n}\frac{1}{2}\sigma_{i,2}^{[\iota]}\mu_2^{[\iota]2} + \sum_{\iota=1}^{n}\left|\varsigma_{i,2}^{[\iota]}\right|\left|\Delta_i^{[\iota]}\right| + \mathcal{F}_i$$

$$(29)$$

The ET control design procedure is now completed. Figure 1 shows a block diagram of the proposed ET control system. The following theorem is provided to summarize the results.

Theorem 1. Under Assumption 1, consider an MAS composed of n-link RMs defined in equation (6), which is supposed to follow a desired reference trajectory over time while trying to keep a predefined formation among the agents. Design the virtual control laws (13) and (28), the adaptive rules (25) and (26). Suppose that the ET control rules are triggered according to equation (27). Then, by applying the control signal $\boldsymbol{u}_i = \mathcal{M}_i\bar{\boldsymbol{u}}_i$ to the ith RM, the following statements hold true

1. For bounded initial conditions (i.e. $q_{i,1}^{[\iota]}(t_0)$, $q_{i,2}^{[\iota]}(t_0)$, $\hat{\mu}_{i,1}^{[\iota]}(t_0)$, and $\hat{\mu}_{i,2}^{[\iota]}(t_0)$), all the resulting closed-loop network signals remain semi-globally uniformly bounded, and the error signals $\boldsymbol{\mathcal{X}}_e = [\boldsymbol{\mathcal{X}}_{1,e}^{\mathrm{T}}, \ldots, \boldsymbol{\mathcal{X}}_{1,e}^{\mathrm{T}}]^{\mathrm{T}}$ with $\boldsymbol{\mathcal{X}}_{i,e}$ defined as

$$\boldsymbol{\mathcal{X}}_{i,e} = \left[\varsigma_{i,1}^{[1]}, \varsigma_{i,1}^{[2]}, \ldots, \varsigma_{i,1}^{[n]}, \varsigma_{i,2}^{[1]}, \varsigma_{i,2}^{[2]}, \ldots, \varsigma_{i,2}^{[n]}\right.$$
$$\left.\tilde{\mu}_{i,1}^{[1]}, \tilde{\mu}_{i,1}^{[2]}, \ldots, \tilde{\mu}_{i,1}^{[n]}, \tilde{\mu}_{i,2}^{[1]}, \tilde{\mu}_{i,2}^{[2]}, \ldots, \tilde{\mu}_{i,2}^{[n]}\right]^{\mathrm{T}}$$

eventually converge to a compact set Ω_s as

$$\Omega_s = \left\{\varsigma_{i,1}^{[\iota]}, \varsigma_{i,2}^{[\iota]}, \tilde{\mu}_{i,1}^{[\iota]}, \tilde{\mu}_{i,2}^{[\iota]}\big| \sum_{i=1}^{N}\sum_{\iota=1}^{n}|\varsigma_{i,1}^{[\iota]}|^2 \leqslant 2\frac{\beta_2}{\beta_1}\right.$$

$$\sum_{i=1}^{N}\sum_{\iota=1}^{n}\mathbf{E}\left[\left|\varsigma_{i,2}^{[\iota]}\right|^4\right] \leqslant 4\frac{\beta_2}{\beta_1}$$

$$\sum_{i=1}^{N}\sum_{\iota=1}^{n}\left|\tilde{\mu}_{i,1}^{[\iota]}\right| \leqslant \sqrt{\gamma_{i,1}^{[\iota]}\frac{\beta_2}{\beta_1}}$$

$$\left.\sum_{i=1}^{N}\sum_{\iota=1}^{n}\left|\tilde{\mu}_{i,2}^{[\iota]}\right| \leqslant \sqrt{\gamma_{i,2}^{[\iota]}\frac{\beta_2}{\beta_1}}\right\}$$
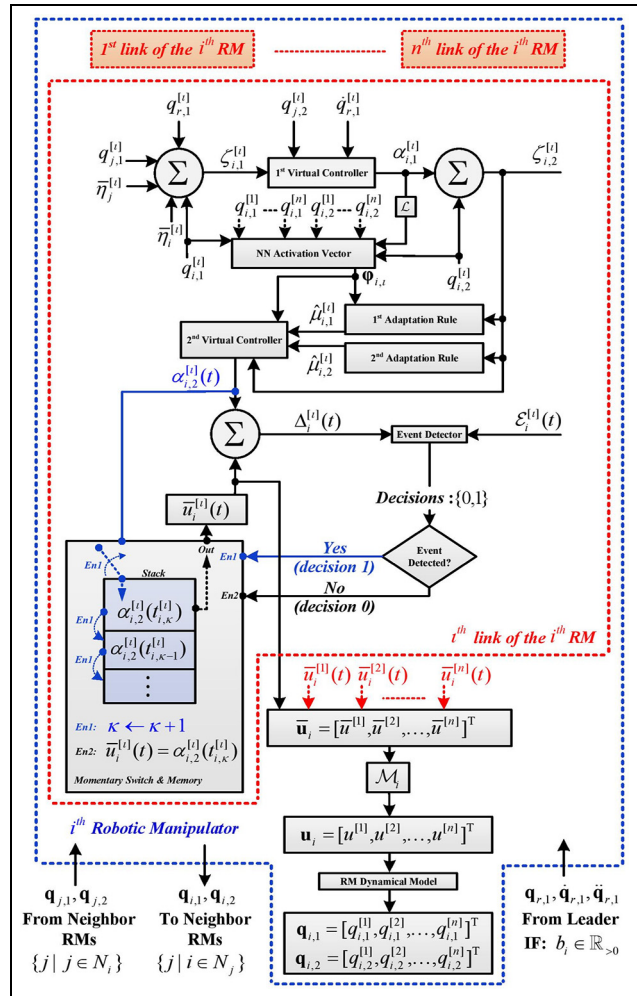
$$(30)$$

where

Figure 1. A block diagram of the proposed ET control system.

$$\beta_1 = \min_{i=1,\ldots,N}\left\{\min_{\iota=1,\ldots,n}\left\{\left[K_{i,1}^{[\iota]} - \frac{d_i + b_i}{2}\right]\right\}\right.$$

$$\min_{\iota=1,\ldots,n}\left\{\left[K_{i,2}^{[\iota]} - \frac{(d_i + b_i)\varepsilon_i^2 + \varepsilon_i^4}{4}\right]\right\}$$

$$\left.\left\{\min_{\iota=1,\ldots,n}\left\{\sigma_{i,1}^{[\iota]}\right\}, \min_{\iota=1,\ldots,n}\left\{\sigma_{i,2}^{[\iota]}\right\}\right\}\right\}$$

and

$$\beta_2 = \sum_{i=1}^{N}\left[\sum_{\iota=1}^{n}\frac{1}{2}\sigma_{i,1}^{[\iota]}\mu_1^{[\iota]2} + \sum_{\iota=1}^{n}\frac{1}{2}\sigma_{i,2}^{[\iota]}\mu_2^{[\iota]2}\right.$$

$$\left. + \sum_{\iota=1}^{n}\frac{3}{4\varepsilon_i^{\frac{4}{3}}}\delta_i^{[\iota]\frac{4}{3}} + \mathcal{F}_i\right]$$

with bounded positive constants $\delta_i^{[\iota]}$ for all $i = 1, \ldots, N$ and $\iota = 1, \ldots, n$.

2. There exist strictly positive parameters $\tilde{t}_i^{[\iota]}$, such that $\{t_{i,\kappa+1}^{[\iota]} - t_{i,\kappa}^{[\iota]} \geq \tilde{t}_i^{[\iota]}\}$ for all $i = 1, \ldots, N$ and $\iota = 1, \ldots, n$, that is, the Zeno phenomenon is excluded for the ETC mechanisms.

Proof. The proof is given in two parts. First, in Part 1, by utilizing Lemma 2 and Definitions 1 and 2, we show that the resulting closed-loop network signals are CSGUUB. Then, in Part 2, we investigate the exclusion of the Zeno phenomenon for the ETC mechanisms.

Part 1. From equation (27), one deduces that $|\Delta_i^{[\iota]}| \leq \mathcal{E}_i^{[\iota]}$. Therefore, according to the properties of $v_{i,1}^{[\iota]}$ and $v_{i,2}^{[\iota]}$, for all $t^{[\iota]} \in [t_{i,\kappa}^{[\iota]}, t_{i,\kappa+1}^{[\iota]})$, one has

$$\left| \Delta_i^{[\iota]} \right| \leq \left| v_{i,1}^{[\iota]} + v_{i,2}^{[\iota]}(t) \right| \equiv \delta_i^{[\iota]}$$

Hence, by applying Young's inequality to $\sum_{\iota=1}^{n} |\zeta_{i,2}^{[\iota]}||\Delta_i^{[\iota]}|$, one has

$$\sum_{\iota=1}^{n} \left| \zeta_{i,2}^{[\iota]} \right| \left| \Delta_i^{[\iota]} \right| \leq \frac{1}{4} \sum_{\iota=1}^{n} \varepsilon_i^4 \zeta_{i,2}^{[\iota]4} + \sum_{\iota=1}^{n} \frac{3}{4\varepsilon_i^{\frac{4}{3}}} \delta_i^{[\iota]\frac{4}{3}}$$

Therefore, equation (29) leads to

$$\begin{aligned}
\mathcal{L}\mathcal{V}_{i,3} \leq &- \sum_{\iota=1}^{n} \left[K_{i,1}^{[\iota]} - \frac{d_i + b_i}{2} \right] \zeta_{i,1}^{[\iota]2} \\
&- \sum_{\iota=1}^{n} \left[K_{i,2}^{[\iota]} - \frac{(d_i + b_i)\varepsilon_i^2 + \varepsilon_i^4}{4} \right] \zeta_{i,2}^{[\iota]4} \\
&- \sum_{\iota=1}^{n} \frac{1}{2} \sigma_{i,1}^{[\iota]} \tilde{\mu}_{i,1}^{[\iota]2} - \sum_{\iota=1}^{n} \frac{1}{2} \sigma_{i,2}^{[\iota]} \tilde{\mu}_{i,2}^{[\iota]2} \\
&+ \sum_{\iota=1}^{n} \frac{1}{2} \sigma_{i,1}^{[\iota]} \mu_1^{[\iota]2} + \sum_{\iota=1}^{n} \frac{1}{2} \sigma_{i,2}^{[\iota]} \mu_2^{[\iota]2} \\
&+ \mathcal{F}_i + \sum_{\iota=1}^{n} \frac{3}{4\varepsilon_i^{\frac{4}{3}}} \delta_i^{[\iota]\frac{4}{3}}
\end{aligned} \tag{31}$$

Now define the total Lyapunov function candidate as

$$\mathcal{V}_T = \sum_{i=1}^{N} \mathcal{V}_{i,3} \tag{32}$$

Taking equation (31) into account, the candidate function equation (32) results in

$$\mathcal{L}\mathcal{V}_T \leq -\beta_1 \mathcal{V}_T + \beta_2 \tag{33}$$

By Lemma 2, one has

$$0 \leq \mathbf{E}[\mathcal{V}_T(\mathcal{X}_e(t))] \leq \mathcal{V}_T(\mathcal{X}_e(t_0))e^{-\beta_1(t-t_0)} + \frac{\beta_2}{\beta_1} \tag{34}$$

This means that

$$\mathbf{E}[\mathcal{V}_T(\mathcal{X}_e(t))] \leq \mathcal{V}_T(\mathcal{X}_e(t_0)) + \frac{\beta_2}{\beta_1}, \forall t > 0 \tag{35}$$

where

$$\begin{aligned}
\mathcal{V}_T(\mathcal{X}_e(t_0)) = &\frac{1}{2} \sum_{i=1}^{N} \sum_{\iota=1}^{n} \zeta_{i,1}^{[\iota]2}(t_0) + \frac{1}{4} \sum_{i=1}^{N} \sum_{\iota=1}^{n} \zeta_{i,2}^{[\iota]4}(t_0) \\
&+ \sum_{i=1}^{N} \sum_{\iota=1}^{n} \frac{1}{2\gamma_{i,1}^{[\iota]}} \tilde{\mu}_{i,1}^{[\iota]2}(t_0) + \sum_{i=1}^{N} \sum_{\iota=1}^{n} \frac{1}{2\gamma_{i,2}^{[\iota]}} \tilde{\mu}_{i,2}^{[\iota]2}(t_0)
\end{aligned}$$

Then, according to equation (35) and the definition of total candidate Lyapunov function equation (32), it can be concluded that all the signals $\zeta_{i,2}^{[\iota]}(t)$ in the closed-loop system are semi-globally uniformly bounded in the sense of the $p = 4$ moment, and signals $\zeta_{i,1}^{[\iota]}(t)$, $\tilde{\mu}_{i,1}^{[\iota]}(t)$, and $\tilde{\mu}_{i,2}^{[\iota]}(t)$ are semi-globally uniformly bounded in mean square (see Definition 1 and Remark 1).

Then, according to Lemma 2, the closed-loop network system has a unique strong solution. From equation (34), the following inequality holds true

$$\lim_{t \to \infty} \mathbf{E}[\mathcal{V}_T(\mathcal{X}_e(t))] \leq \frac{\beta_2}{\beta_1}$$

Then, the error signals $\mathcal{X}_e$ eventually converge to a compact set Ω_s defined in equation (30). Therefore, by Part 1, we have proved that the resulting closed-loop network signals are CSGUUB. As a result, the predefined formation among the RM agents is satisfied according to Definition 2. We have to note that by choosing appropriate control gains (i.e. $K_{i,1}^{[\iota]}$ and $K_{i,2}^{[\iota]}$) and design parameters (for instance, $\sigma_{i,1}^{[\iota]}$, $\sigma_{i,2}^{[\iota]}$, $\gamma_{i,1}^{[\iota]}$, $\gamma_{i,2}^{[\iota]}$, etc.), β_1 can be made arbitrarily large and β_2 can be made arbitrarily small. This certainly affects the compact set in equation (30).

Part 2. We know that $\forall t^{[\iota]} \in [t_{i,\kappa}^{[\iota]}, t_{i,\kappa+1}^{[\iota]})$, the control measurement error is defined as $\Delta_i^{[\iota]}(t) = \bar{u}_i^{[\iota]}(t) - \alpha_{i,2}^{[\iota]}(t)$. Then, one has

$$\frac{\mathrm{d}}{\mathrm{d}t} \left| \Delta_i^{[\iota]}(t) \right| = \text{sign}\left(\alpha_{i,2}^{[\iota]}(t) \right) \dot{\alpha}_{i,2}^{[\iota]}(t) \leq \left| \dot{\alpha}_{i,2}^{[\iota]}(t) \right| \tag{36}$$

According to the aforementioned discussion in Part 1 of the proof, and since $\dot{\alpha}_{i,2}^{[\iota]}(t)$ is differentiable and

continuous, there exists a positive constant $\bar{\delta}_i^{[\iota]}$ such that $|\dot{\alpha}_{i,2}^{[\iota]}(t)| \leqslant \bar{\delta}_i^{[\iota]}$. We know that $\Delta_i^{[\iota]}(t_{i,\kappa}) = 0$. Therefore, it can be verified that $\lim_{t \to t_{i,\kappa+1}^{[\iota]}} \Delta_i^{[\iota]} = \mathcal{E}_i^{[\iota]}$, and therefore, $\tilde{t}_i^{[\iota]} \geqslant \mathcal{E}_i^{[\iota]} / \bar{\delta}_i^{[\iota]}$. By Part 2, we have proved that the Zeno phenomenon is excluded for the ETC mechanisms.

By Parts I and II, the proof is completely given. ∎

Simulation results

To investigate the effectiveness of the proposed approach, in this section, we conduct simulations over a networked system of RMs with different purposes in sequential subsections. First, the proposed method is applied to satisfy the formation of $N = 3$ identical RMs according to the dynamics in equation (6). Second, the numerical specification of the executed events is investigated in two parts. Then, the proposed approach in this article is compared to the studied method in Xu et al.[29] to show that when the external disturbances are considered stochastic, the deterministic control schemes fail to show an appropriate performance. Then, we show the effectiveness of our studied method in terms of reducing the total number of events. Finally, the rule of thumb to choose the control gains, adaptation design constants, and other parameters is presented.

The formation of multiple RMs

In order to illustrate the efficiency of our proposed ETC approach, the simulations are performed on a networked group of $N = 3$, two-link identical RMs (see Figure 2) subject to stochastic environmental loads described by equation (6). We have $\boldsymbol{q}_{i,1} = [q_{i,1}^{[1]}, q_{i,1}^{[2]}]^{\mathrm{T}} \in \mathbb{R}^2$ and $\boldsymbol{q}_{i,2} = [q_{i,2}^{[1]}, q_{i,2}^{[2]}]^{\mathrm{T}} \in \mathbb{R}^2$.

For the ith follower RM, the model parameters are borrowed from Loria and Nijmeijer.[40] The inertia matrix $\boldsymbol{\mathcal{M}}_i$ is denoted as

$$\boldsymbol{\mathcal{M}}_i = \begin{bmatrix} c_1 + 2c_2 \cos\left(q_{i,1}^{[2]}\right) & c_3 + c_2 \cos\left(q_{i,1}^{[2]}\right) \\ c_3 + c_2 \cos\left(q_{i,1}^{[2]}\right) & c_4 \end{bmatrix}$$

Furthermore, the total Coriolis and centripetal acceleration matrix is

$$\boldsymbol{C}_i\left(\boldsymbol{q}_{i,1}, \boldsymbol{q}_{i,2}\right)$$
$$= \begin{bmatrix} -c_2 \sin\left(q_{i,1}^{[2]}\right) q_{i,2}^{[2]} & -c_2 \sin\left(q_{i,1}^{[2]}\right)\left(q_{i,2}^{[1]} + q_{i,2}^{[2]}\right) \\ c_2 \sin\left(q_{i,1}^{[2]}\right) q_{i,2}^{[1]} & 0 \end{bmatrix}$$

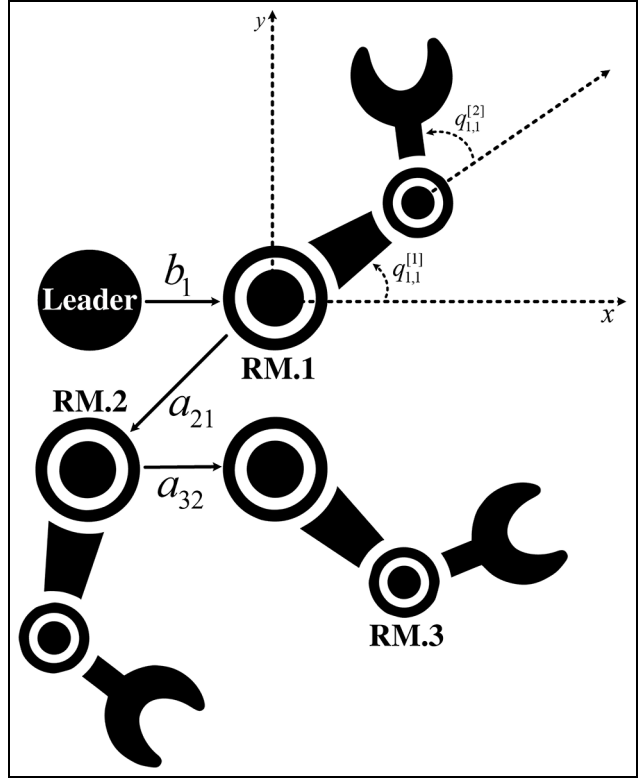The damping matrix and the gravity effect vector are also as follows

Figure 2. The graph communication and diagram of two-link prototype RMs.

$$\boldsymbol{G}_i\left(\boldsymbol{q}_{i,1}\right) = \begin{bmatrix} c_5 \sin\left(q_{i,1}^{[1]}\right) + c_6 \sin\left(q_{i,1}^{[1]} + q_{i,1}^{[2]}\right) \\ c_6 \sin\left(q_{i,1}^{[1]} + q_{i,1}^{[2]}\right) \end{bmatrix},$$
$$\boldsymbol{D}_i\left(\boldsymbol{q}_{i,1}\right) = \begin{bmatrix} c_7 & 0 \\ 0 & c_8 \end{bmatrix}$$

where $c_1 = 8.77\,\mathrm{kgm}^2$, $c_2 = 0.51\,\mathrm{kgm}^2$, $c_3 = 0.76\,\mathrm{kgm}^2$, $c_4 = 0.62\,\mathrm{kgm}^2$, $c_5 = 74.48\,\mathrm{Nm}$, $c_6 = 6.174\,\mathrm{Nm}$, $c_7 = 2.3\,\mathrm{Nms}$, and $c_8 = 0.17\,\mathrm{Nms}$. In addition, $\boldsymbol{\mathcal{G}}_i(\boldsymbol{q}_{i,2}, t) = [0.1q_{i,2}^{[2]} \sin(q_{i,2}^{[1]}), 0.1q_{i,2}^{[1]} \cos(q_{i,2}^{[2]})]^{\mathrm{T}}$.

The RM agents are supposed to follow a desired trajectory as $\boldsymbol{q}_{r,1} = [\sin(t), \cos(t)]^{\mathrm{T}}$, while trying to keep a predefined formation among themselves according to the upcoming parameters. For the ith agent, the predetermined desired formation position with respect to the leader is denoted by $\bar{\boldsymbol{\eta}}_i \in \mathbb{R}^2$. In the simulation results, we choose $\bar{\boldsymbol{\eta}}_1 = [1, -1]^{\mathrm{T}}$, $\bar{\boldsymbol{\eta}}_2 = [2, -2]^{\mathrm{T}}$, and $\bar{\boldsymbol{\eta}}_3 = [0, -1]^{\mathrm{T}}$.

The agents are initially stationary positioned at $q_{1,1}^{[1]}(0) = 0$, $q_{2,1}^{[1]}(0) = 0$, $q_{3,1}^{[1]}(0) = 0$, $q_{1,1}^{[2]}(0) = 1$, $q_{2,1}^{[2]}(0) = 1$, and $q_{3,1}^{[2]}(0) = 1$. The approximated parameters are also initially set to zero. The simulation is performed with a time step of $T = 5\,\mathrm{ms}$ (As a trade-off,
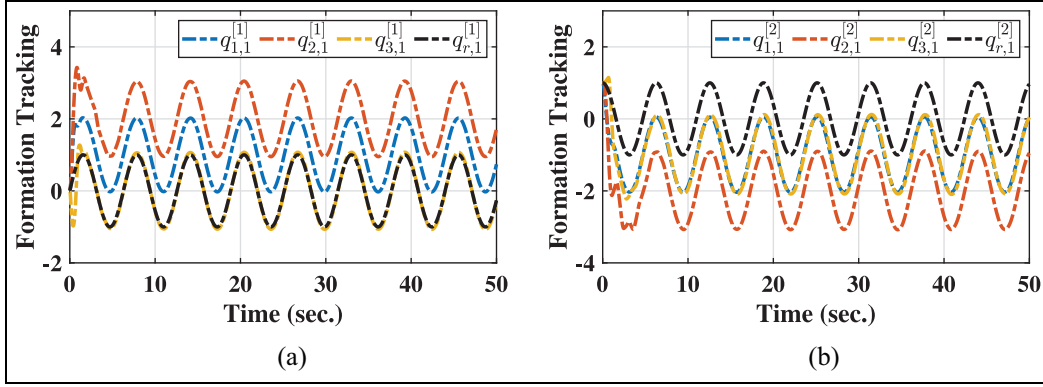
Figure 3. Trajectory tracking of (a) $q_{i,1}^{[1]}$ with respect to $q_{r,1}^{[1]}$ and (b) $q_{i,1}^{[2]}$ with respect to $q_{r,1}^{[2]}$.
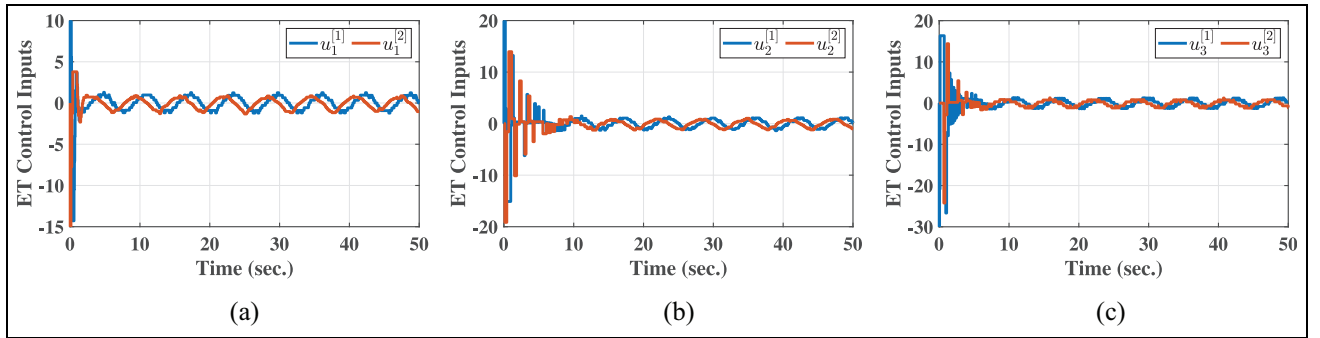

Figure 4. Control input (a) $u_1^{[\iota]}$, (b) $u_2^{[\iota]}$, and (c) $u_3^{[\iota]}$, $\iota = 1, 2$.

referring to some literature, the authors choose $T = 5\,\text{ms}$ as the sample time step. We investigated in details the impact of changing the sampling time step on the closed-loop system performance in the upcoming sections of the simulation results.). The proposed method is evaluated in a 50-s simulation run-time.

The control gains are also selected as $K_{i,1}^{[1]} = 4$, $K_{i,1}^{[2]} = 3$, $K_{i,2}^{[1]} = 5$, and $K_{i,2}^{[2]} = 4$. In addition, $v_{1,1}^{[\iota]} = 0.25$, $v_{2,1}^{[\iota]} = 0.5$, and $v_{3,1}^{[\iota]} = 0.5$ for $\iota = 1, 2$. Furthermore, $v_{1,2}^{[\iota]}(t) = 3\exp(-0.2t)$, $v_{2,2}^{[\iota]}(t) = 3\exp(-0.4t)$, and $v_{3,2}^{[\iota]}(t) = 4\exp(-0.8t)$ for $\iota = 1, 2$.

Figures 3–9 show the results including tracking formation performance, control inputs, the inter-event times, and the adaptive parameters for the proposed ETC scheme. It can be seen from Figure 3 that the follower agents are showing an acceptable tracking performance while keeping the desired formation among themselves. The ET control inputs are also depicted in Figure 4. The executed events for all the agents are also depicted in Figures 5–7. Furthermore, the adaptive parameters are shown in Figures 8 and 9.

Quantitative analysis

In this section, we report the numerical specifications of the executed events in two parts. First, the results of applying Theorem 1 with a sampling time step of $T = 5\,\text{ms}$ are reported in terms of the minimum and maximum inter-event times in addition to the total number of events and the average inter-event times for each link of all the RM agents. Second, the impact of increasing the sampling time step on the executed events is studied while the system gains and parameters kept unchanged.

Numerical specifications of the executed events. Based on 100 simulation tests, the average values of some important indices are reported in this section. More understandably, the numerical specifications of the executed events during the simulation time are averagely reported in Table 1 with respect to Theorem 1 and a sampling time step of $T = 5\,\text{ms}$ over 100 simulation tests (The used notations in Tables 1 and 2; $\mathcal{C}$olumn.1: $\mathcal{A}[\text{Min}(t_{i,\kappa+1}^{[\iota]} - t_{i,\kappa}^{[\iota]})]$, $\mathcal{C}$olumn.2: $\mathcal{A}[\text{Max}(t_{i,\kappa+1}^{[\iota]} - t_{i,\kappa}^{[\iota]})]$, $\mathcal{C}$olumn.3: $\mathcal{A}[\text{AIE}]$, and $\mathcal{C}$olumn.4: $\mathcal{A}[\text{TNE}]$. AIE: average inter-event time, TNE: total number of events, and $\mathcal{A}[\bullet]$: the average value of performing a predefined number of tests.). We have to note that, for example, in Table 1, by $\mathcal{A}[\text{Min}(t_{i,\kappa+1}^{[\iota]} - t_{i,\kappa}^{[\iota]})]$, we mean the average value of the minimum inter-event times over performing a 100 number of tests for each link of all the RM followers.

From Table 1, we see that the average inter-event time among all the follower agents is approximately 50 times larger than the system sampling time step. The
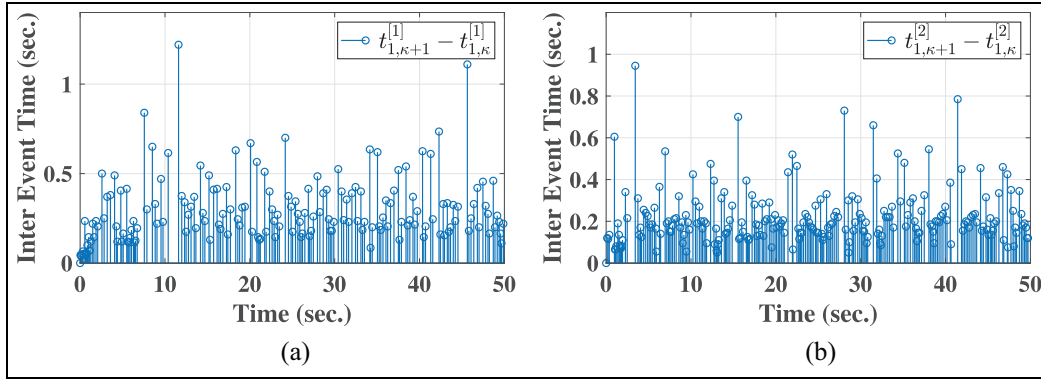
Figure 5. Controller inter-event times (a) $t_{1,\kappa+1}^{[1]} - t_{1,\kappa}^{[1]}$ and (b) $t_{1,\kappa+1}^{[2]} - t_{1,\kappa}^{[2]}$.
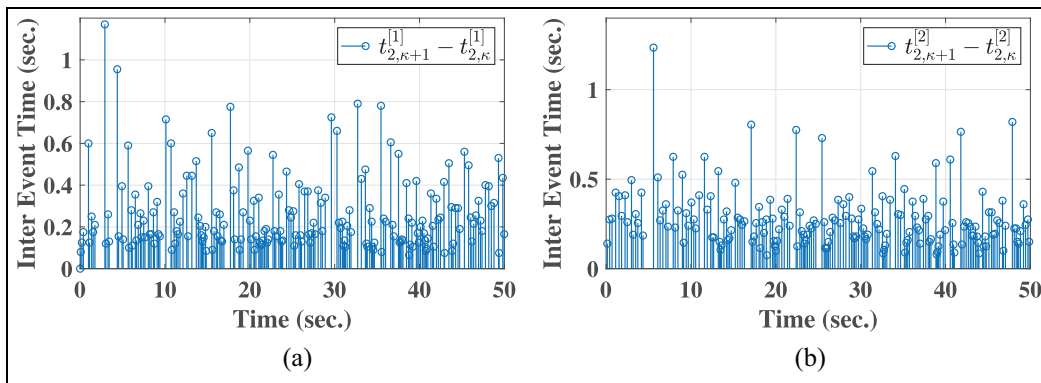

Figure 6. Controller inter-event times (a) $t_{2,\kappa+1}^{[1]} - t_{2,\kappa}^{[1]}$ and (b) $t_{2,\kappa+1}^{[2]} - t_{2,\kappa}^{[2]}$.
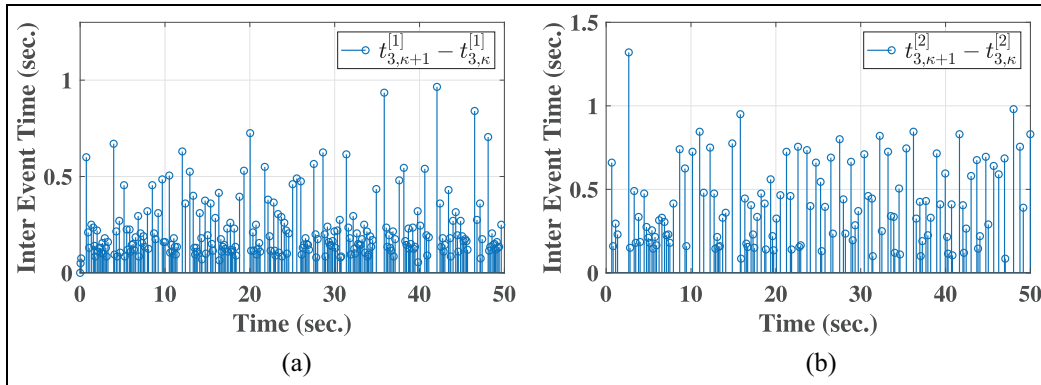

Figure 7. Controller inter-event times (a) $t_{3,\kappa+1}^{[1]} - t_{3,\kappa}^{[1]}$ and (b) $t_{3,\kappa+1}^{[2]} - t_{3,\kappa}^{[2]}$.

total number of events for all the followers is also reported in Table 1, where we can see that the control updates are respectively provoked 172, 239, 196, 181, 227, and 128 times out of 10,000 possible instants. We also infer from Table 1 that the agents have a minimum of 8, 10, 12, 14, 10, and 16 sample-times hibernate period of time during the simulation run. A maximum time interval of rest is also reported for all follower agents in Table 1, where we observe that RM links experience 244, 188, 236, 250, 193, and 264 sample-times inactive, respectively.

The impact of changing the sampling time step. Next, we investigate the impact of increasing the sampling time step on the executed events and systems performance while the system parameters kept unchanged. The numerical specifications of the executed events during the simulation time are averagely reported in Table 2 with respect to Theorem 1 and sampling time steps $T = 10$ ms and $T = 20$ ms over 100 simulation tests. We see from Table 2 that by increasing the sample time of system, the total number of events remained almost unchanged. In addition, we infer from Tables 1 and 2
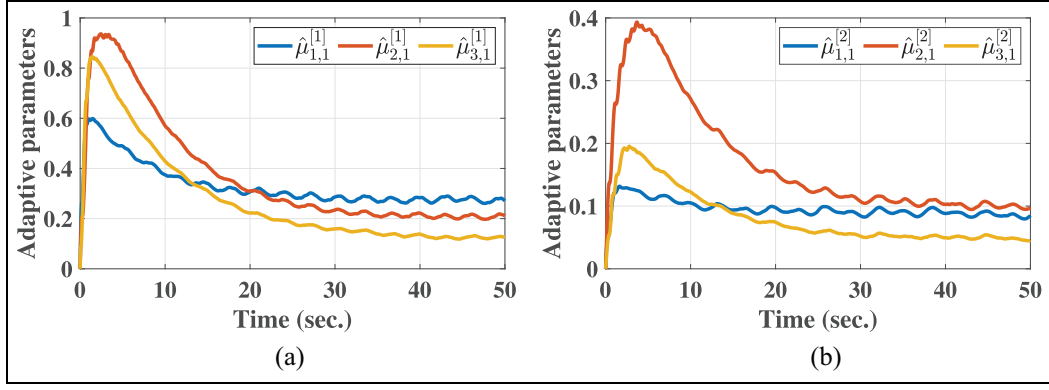
Figure 8. Adaptive parameters (a) $\hat{\mu}_{i,1}^{[1]}$ and (b) $\hat{\mu}_{i,1}^{[2]}$.
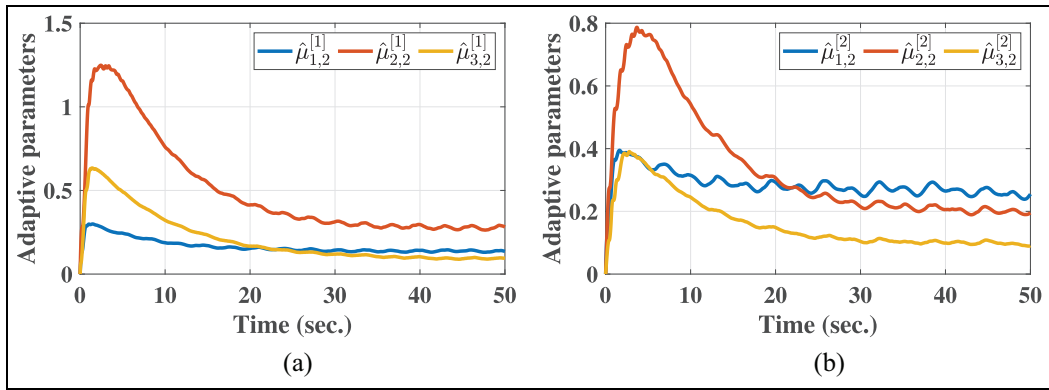

Figure 9. Adaptive parameters (a) $\hat{\mu}_{i,2}^{[1]}$ and (b) $\hat{\mu}_{i,2}^{[2]}$.

Table 1. Numerical specifications of the executed events for $\iota = 1, 2$ and $i = 1, 2, 3$ over 100 simulation tests.

| | Time step: $T = 5$ ms | | | |
	$\mathcal{C}$olumn.1	$\mathcal{C}$olumn.2	$\mathcal{C}$olumn.3	$\mathcal{C}$olumn.4
First RM	0.04	1.22	0.2853	172
	0.05	0.94	0.2158	239
Second RM	0.06	1.18	0.2555	196
	0.07	1.235	0.2732	181
Third RM	0.05	0.963	0.2161	227
	0.08	1.32	0.3991	128

RM: robotic manipulator.

Table 2. Numerical specifications of the executed events for $\iota = 1, 2$ and $i = 1, 2, 3$ over 100 simulation tests.

| | Time step: $T = 10$ ms | | | |
	$\mathcal{C}$olumn.1	$\mathcal{C}$olumn.2	$\mathcal{C}$olumn.3	$\mathcal{C}$olumn.4
First RM	0.04	1.12	0.2516	175
	0.04	0.88	0.2010	241
Second RM	0.06	0.95	0.2270	202
	0.08	1.05	0.2653	182
Third RM	0.06	0.85	0.2014	238
	0.07	1.19	0.3577	132

| | Time step: $T = 20$ ms | | | |
	$\mathcal{C}$olumn.1	$\mathcal{C}$olumn.2	$\mathcal{C}$olumn.3	$\mathcal{C}$olumn.4
First RM	0.04	0.90	0.2184	179
	0.06	0.98	0.1911	247
Second RM	0.06	0.92	0.2012	206
	0.08	1.32	0.2572	187
Third RM	0.06	1.36	0.1990	236
	0.08	1.58	0.3259	135

RM: robotic manipulator.

that the minimum inter-event intervals remain almost the same regardless of increasing the sampling time step.

The average total absolute error (i.e. $\mathcal{A}[\sum_{\iota=1}^{2} \sum_{k=1}^{p} |\varsigma_{i,1}^{[\iota]}(k)|]$ for $\iota = 1, 2$, where p is the total number of time steps) index is also employed for each RM agent to better clarify the effectiveness of our proposed design in terms of tracking performance with different sampling times. It can be seen from Table 3 that the tracking performance of the proposed approach in this article is remained almost the same

regardless of changing the sampling time step in the simulation results. To be precise, by increasing the time

Table 3. Numerical specifications of the average values of total absolute error index for $i = 1, 2, 3$ over 100 simulation tests.

	$\mathcal{A}[\sum_{\iota=1}^{2} \sum_{k=1}^{p} \|\zeta_{i,1}^{[\iota]}(k)\|]$		
	$T = 5$ ms	$T = 10$ ms	$T = 20$ ms
First RM	≈ 163	≈ 164	≈ 163
Second RM	≈ 215	≈ 214	≈ 214
Third RM	≈ 300	≈ 298	≈ 299

RM: robotic manipulator.

Table 4. Numerical specifications of the average values of total absolute error index for $i = 1, 2, 3$ over 100 simulation tests; the proposed method in this article versus the studied method in Xu et al.[29]

	$\mathcal{A}[\sum_{\iota=1}^{2} \sum_{k=1}^{p} \|\zeta_{i,1}^{[\iota]}(k)\|]$ and $T = 10$ ms	
	This article	Xu et al.[29]
First RM	≈ 161	≈ 340
Second RM	≈ 214	≈ 494
Third RM	≈ 299	≈ 608

RM: robotic manipulator.

step from $T = 5$ ms to $T = 20$ ms, the tracking performance remains acceptable and almost unchanged. Consequently, changing the time step does not affect the closed-loop system performance with respect to the control objectives. Furthermore, the smaller the sample time is, the discrete simulation effect is much more similar to the continuous simulation effect, and the obtained data are smoother. However, the longer the sample time is, the calculation time is less, which results in saving the computing resources.

To recapitulate, regardless of the value that the sampling time step T is taken, the inter-event intervals are always sub-multiples of the sampling time step. Other words, we always have $t_{i,\kappa+1}^{[\iota]} - t_{i,\kappa}^{[\iota]} = n^{+}T$, where n^{+} is an integer that satisfies the exclusion of Zeno phenomenon according to the second part of Theorem 1. Overall, we infer from this section that with all the sampling time steps $T = 5$ ms, $T = 10$ ms, and $T = 20$ ms, the total number of event execution times is averagely 190, 195, and 200 instants out of 10^{4}, 5000, and 2500 possible samples. This shows that the proposed ET control approach is efficient in providing an appropriate performance in terms of reducing the number of control updates with respect to the possible number of updates in time-triggered frameworks regardless of the chosen sampling time step.

Comparison with the existing results

In this section, we perform the simulations to compare our proposed method with the existing method in Xu et al.[29] for the cooperative control of RM-MASs. We evaluate if the proposed method in this article shows an acceptable performance in terms of reducing the number of control input updates and handling the stochastic environmental loads. To be fair, we have generalized the proposed approach in this article to consider the tracking consensus problem of multiple RMs. To this end, the predetermined desired formation orientation and position with respect to the leader is set to $\bar{\eta}_i = [0, 0]^T$ for all $i = 1, 2, 3$. A virtual leader is also considered for both the algorithms as $q_{r,1} = [\sin(t), \cos(t)]^T$. The network topology is also chosen as denoted in Figure 2. The priory identified system parameters are also chosen the same as defined earlier in this article. The initial conditions are also

chosen the same for both algorithms in this article and the proposed method in Xu et al.[29]

Stochastic environmental disturbances impact. In this section, we compare our proposed method with the deterministic control design in Xu et al.[29] in terms of the effectiveness of the stochastic scheme in providing an appropriate performance in tracking the desired trajectory among the RMs. A vector of deterministic and bounded external disturbances is considered and compensated in Xu et al.[29] However, to show the impact of stochastic external disturbance denoted by standard Wiener process, the proposed algorithm in Xu et al.[29] is applied on the stochastic dynamics defined in equation (6). The same stochastic external disturbance functions are also applied to both algorithms in this article and the proposed method in Xu et al.[29]

Regardless of the executed events, in this part, we just want to study the way that the external disturbances affect the closed-loop system performance. The simulation is performed for 50 s with a time step of $T = 10$ ms. Once again, the average total absolute error (i.e. $\mathcal{A}[\sum_{\iota=1}^{2} \sum_{k=1}^{p} \|\zeta_{i,1}^{[\iota]}(k)\|]$ for $\iota = 1, 2$) index is employed for each RM agent to better clarify the applicability of the investigated design approaches in terms of handling the external stochastic disturbances with respect to the tracking performance. The results are reported in Table 4.

We see that the tracking performance of our proposed approach is more acceptable compared to the studied method in Xu et al.[29] The reported results in Table 4 show a poor tracking performance for the deterministic control architecture. We infer that the closed-loop system is unable to track the reference trajectory and the consensus is not acceptably realized with the studied method in Xu et al.[29]

Compared to the proposed method in this article, a great amount of control effort is also required for deterministic control design to even avoid instability, regardless of unsatisfactory tracking performance. We have to note that with very large values of control gains, the closed-loop system even leads to instability with the investigated method in Xu et al.[29] We see from the

Table 5. Numerical specifications of the average values of total absolute control index for $i = 1, 2, 3$ over 100 simulation tests; the proposed method in this article versus the studied method in Xu et al.[29]

| | $\mathcal{A}[\sum_{\iota=1}^{2} \sum_{\kappa=1}^{p} |u_i^{[\iota]}(\kappa)|]$ and $T = 10$ ms | |
	This article	Xu et al.[29]
First RM	$\approx 4.1 \times 10^3$	$\approx 5.4 \times 10^3$
Second RM	$\approx 5.4 \times 10^3$	$\approx 4.5 \times 10^3$
Third RM	$\approx 6.2 \times 10^3$	$\approx 10.3 \times 10^3$

RM: robotic manipulator.

Table 6. The total number of events for $i = 1, 2, 3$; the proposed method in this article versus the studied method in Xu et al.[29]

| | Total number of events | |
	This article	Xu et al.[29]
First RM	165 + 235	2×265
Second RM	194 + 179	2×281
Third RM	224 + 128	2×274

RM: robotic manipulator.

simulation results that the deterministic control architectures are often not applicable in stochastic cases.

To further explain the effects of stochastic environmental loads on the performance of deterministic control designs, the average values of total absolute control input in possible directions (i.e. $\mathcal{A}[\sum_{\iota=1}^{2} \sum_{\kappa=1}^{p} |u_i^{[\iota]}(\kappa)|]$) are calculated for both methods based on 100 simulation tests. This indicates the expected closed-loop system energy consumption for the investigated approaches. The numerical results of average total absolute control index are reported in Table 5. We see from Table 5 that a larger expected amount of control effort is required for deterministic control design to avoid instability, while the proposed method in this article requires reasonable deals of energy (compared to Xu et al.[29]) to keep the consensus among the RM agents and force the group to track the desired trajectory.

Simultaneous update of control links impact. As we mentioned earlier, this is the first instance that the ET mechanisms are designed such that each manipulating link can independently update its actuator according to a triggering condition regardless of the value and update instants of other links. More precisely, a total number of two triggering thresholds are introduced for each follower RM in the simulation results that are working independently for all the agents. The studied method in Xu et al.[29] has an ET framework in which all the n links should be updated simultaneously. In order to investigate the effectiveness of our proposed approach in terms of reducing the number of actuator updates by introducing separate update rules, the simulation is again performed for 50 s with a time step of $T = 10$ ms. This time, the stochastic and deterministic disturbances are removed from the dynamics in both methods.

The total number of events is reported in Table 6 for both algorithms in this article and the studied method in Xu et al.[29] Although that the numerical specification of the executed events in Table 6 shows a fewer number of total triggering instants for the actuator links for our proposed method compared to Xu et al.,[29] this does not

show the deficiency of the studied architecture in Xu et al.[29]

The number of executed events is larger for the studied ET control method in Xu et al.[29] compared to our proposed approach; however, the tracking performance of Xu et al.[29] is fairly more acceptable. This is obviously true due to the fact that the actuators tend to be updated faster. To recapitulate, our proposed method saved more energy resources at the expense of less tracking performance. This is not surprising because that choosing the control objectives in each framework is a compromise between lots of factors.

Parameter tuning guideline

The rule of thumb to choose the control gains, adaptation design constants, and other parameters is as follows:

R1: the control gains $K_{i,1}^{[\iota]}$, $K_{i,2}^{[\iota]}$ and design parameters ε_i must be chosen such that $[K_{i,1}^{[\iota]} - d_i + b_i/2]$ and $[K_{i,2}^{[\iota]} - (d_i + b_i)\varepsilon_i^2 + \varepsilon_i^4/4]$ are strictly positive constants for all $i = 1, \ldots, N$ and $\iota = 1, \ldots, n$.
R2: increasing the control gains $K_{i,1}^{[\iota]}$ and $K_{i,2}^{[\iota]}$ results in faster transient response. This choice, however, increases the control effort, see equations (28) and (31).
R3: the larger value of ε_i is, the smaller the tracking errors are according to equation (34) and the terms of β_2. However, ε_i should not be selected such that $(d_i + b_i)\varepsilon_i^2 + \varepsilon_i^4/4$ tends to the value of $K_{i,2}^{[\iota]}$.
R4: based on the definition of $\mathcal{F}_i$ in equation (24), and according to equation (34) and the terms of β_2, small values of $\varpi_{i,1}$ and $\varpi_{i,2}$ (as well as $\sigma_{i,1}^{[\iota]}$ and $\sigma_{i,2}^{[\iota]}$) also result in small tracking errors.
R5: the robustness of the proposed controller can be improved by increasing the values of $\gamma_{i,1}^{[\iota]}$ and $\gamma_{i,2}^{[\iota]}$ for all $i = 1, \ldots, N$ and $\iota = 1, \ldots, n$. However, these values are not allowed to be very large constants because the closed-loop system fails in preserving the stability.

The aforementioned guideline is a matter of trial and error. It is not supposed to be an optimal way of choosing the design gains and parameters. The user is in charge of tuning the parameters according to above rules until an acceptable performance is achieved which seems satisfactory regarding the control objectives. To

recapitulate, the control gains and design parameters are better to be selected such that β_1 is made sufficiently large and β_2 is made acceptably small according to equation (34).

Conclusion and future directions

The tracking formation performance for a group of uncertain non-linear *n*-link RM-MASs is considered in this article by proposing a fully distributed ET control framework and utilizing the backstepping approach. The non-linear RM-MASs are subject to stochastic environmental loads. By introducing extra virtual controllers in the final step of the backstepping design, ET mechanisms are introduced for each agent to update its control input in a fully distributed manner. A rigorous proof of the convergence of all the closed-loop signals in probability is then given and the Zeno phenomenon is excluded for the control ET architectures. The simulation experiments finally quantify the effectiveness of proposed approach in terms of reducing the number of control updates and handling the external disturbances.

One of the main recent concerns in NCSs is the security of implementation and its resilience to different types of cyber attacks which impact the expected performance of practical systems. In future, we investigate resilience of the proposed implementation under different cyber attacks such as the denial of service (DoS).

ORCID iD

Ali Azarbahram (iD) https://orcid.org/0000-0002-3341-4037

References

1. Li Z, Wen G, Duan Z, et al. Designing fully distributed consensus protocols for linear multi-agent systems with directed graphs. *IEEE T Automat Contr* 2015; 60(4): 1152–1157.
2. Li Z, Ren W, Liu X, et al. Distributed consensus of linear multi-agent systems with adaptive dynamic protocols. *Automatica* 2013; 49(7): 1986–1995.
3. Krstic M, Kanellakopoulos I and Kokotovic PV. *Nonlinear and adaptive control design*. New York: Wiley, 1995.
4. Yao Q. Adaptive trajectory tracking control of a free-flying space manipulator with guaranteed prescribed performance and actuator saturation. *Acta Astronaut* 2021; 185: 283–298.
5. Aghaei VT, Ağababaoğlu A, Yıldırım S, et al. A real-world application of Markov chain Monte Carlo method for Bayesian trajectory control of a robotic manipulator. *ISA T*. Epub ahead of print 9 June 2021. DOI: 10.1016/j.isatra.2021.06.010.
6. Shojaei K, Kazemy A and Chatraei A. An observer-based neural adaptive PID^2 controller for robot manipulators including motor dynamics with a prescribed performance. *IEEE/ASME T Mech* 2021; 26(3): 1689–1699.
7. Oh KK, Park MC and Ahn HS. A survey of multi-agent formation control. *Automatica* 2015; 53: 424–440.
8. Qin J, Ma Q, Shi Y, et al. Recent advances in consensus of multi-agent systems: a brief survey. *IEEE T Ind Electron* 2017; 64(6): 4972–4983.
9. Meng Z, Ren W and You Z. Distributed finite-time attitude containment control for multiple rigid bodies. *Automatica* 2010; 46(12): 2092–2099.
10. Mei J, Ren W and Ma G. Distributed containment control for Lagrangian networks with parametric uncertainties under a directed graph. *Automatica* 2012; 48(4): 653–659.
11. Shahvali M and Shojaei K. Distributed control of networked uncertain Euler–Lagrange systems in the presence of stochastic disturbances: a prescribed performance approach. *Nonlinear Dynam* 2017; 90(1): 697–715.
12. Wu B, Lemmon MD and Lin H. Formal methods for stability analysis of networked control systems with IEEE 802.15.4 protocol. *IEEE T Contr Syst T* 2018; 26(5): 1635–1645.
13. Girard A. Dynamic triggering mechanisms for event-triggered control. *IEEE T Automat Contr* 2015; 60(7): 1992–1997.
14. Dimarogonas DV, Frazzoli E and Johansson KH. Distributed event-triggered control for multi-agent systems. *IEEE T Automat Contr* 2012; 57(5): 1291–1297.
15. Kumari K, Behera AK and Bandyopadhyay B. Event-triggered sliding mode-based tracking control for uncertain Euler–Lagrange systems. *IET Control Theory A* 2018; 12(9): 1228–1235.
16. Diao S, Sun W, Su SF, et al. Adaptive fuzzy event-triggered control for single-link flexible-joint robots with actuator failures. *IEEE T Cybernetics*. Epub ahead of print 27 January 2021. DOI: 10.1109/TCYB.2021.3049536.
17. Bu W, Li T, Yang J, et al. Disturbance observer–based event-triggered tracking control of networked robot manipulator. *Meas Control* 2020; 53: 892–898.
18. Li H, Liao X, Huang T, et al. Event-triggering sampling based leader-following consensus in second-order multi-agent systems. *IEEE T Automat Contr* 2015; 60(7): 1998–2003.
19. Hu W, Liu L and Feng G. Consensus of linear multi-agent systems by distributed event-triggered strategy. *IEEE T Cybernetics* 2016; 46(1): 148–157.
20. Wang L, Dong J and Xi C. Event-triggered adaptive consensus for fuzzy output-constrained multi-agent systems with observers. *J Frankl Inst* 2020; 357(1): 82–105.

21. Zhou Q, Wang W, Ma H, et al. Event-triggered fuzzy adaptive containment control for nonlinear multiagent systems with unknown Bouc–Wen hysteresis input. *IEEE T Fuzzy Syst* 2021; 29: 731–741.
22. Zhou Q, Wang W, Liang H, et al. Observer-based event-triggered fuzzy adaptive bipartite containment control of multiagent systems with input quantization. *IEEE T Fuzzy Syst* 2021; 29: 372–384.
23. Zhang Y, Wang D, Peng Z, et al. Event-triggered ISS-modular neural network control for containment maneuvering of nonlinear strict-feedback multi-agent systems. *Neurocomputing* 2020; 377: 314–324.
24. Wang W, Li Y and Tong S. Neural-network-based adaptive event-triggered consensus control of nonstrict-feedback nonlinear systems. *IEEE T Neur Net Lear* 2021; 32(4): 1750–1764.
25. Patel K and Mehta A. Discrete-time event-triggered higher order sliding mode control for consensus of 2-DOF robotic arms. *Eur J Control* 2020; 56: 231–241.
26. Liu Q, Ye M, Qin J, et al. Event-triggered algorithms for leader–follower consensus of networked Euler–Lagrange agents. *IEEE T Syst Man Cy: S* 2019; 49(7): 1435–1447.
27. Yao XY, Ding HF, Ge MF, et al. Event-triggered synchronization control of networked Euler–Lagrange systems without requiring relative velocity information. *Inform Sciences* 2020; 508: 183–199.
28. Xu T, Duan Z, Sun Z, et al. Distributed event-triggered tracking control with a dynamic leader for multiple Euler–Lagrange systems under directed networks. *Int J Robust Nonlin* 2020; 30(8): 3073–3093.
29. Xu T, Duan Z and Sun Z. Event-based distributed robust synchronization control for multiple Euler–Lagrange systems without relative velocity measurements. *Int J Robust Nonlin* 2019; 29(11): 3684–3700.
30. Qin D, Liu A, Zhang D, et al. Formation control of mobile robot systems incorporating primal-dual neural network and distributed predictive approach. *J Frankl Inst* 2020; 357(17): 12454–12472.
31. Shojaei K. Neural adaptive PID formation control of car-like mobile robots without velocity measurements. *Adv Robotics* 2017; 31(18): 947–964.
32. Long J, Wang W, Liu K, et al. Adaptive time-varying formation control of uncertain Euler–Lagrange systems with event-triggered communication. *Int J Robust Nonlin* 2021; 31: 9026–9039.
33. Chen L, Li C, Xiao B, et al. Formation-containment control of networked Euler–Lagrange systems: an event-triggered framework. *ISA T* 2019; 86: 87–97.
34. Chu X, Peng Z, Wen G, et al. Distributed formation tracking of multi-robot systems with nonholonomic constraint via event-triggered approach. *Neurocomputing* 2018; 275: 121–131.
35. Li Y, Qiang S, Zhuang X, et al. Robust and adaptive backstepping control for nonlinear systems using RBF neural networks. *IEEE T Neural Networ* 2004; 15(3): 693–701.
36. Do K. Control of fully actuated ocean vehicles under stochastic environmental loads in three dimensional space. *Ocean Eng* 2015; 99: 34–43.
37. Wang H, Liu X and Liu K. Robust adaptive neural tracking control for a class of stochastic nonlinear interconnected systems. *IEEE T Neur Net Lear* 2016; 27(3): 510–523.
38. Karatzas I, Karatzas J and Shreve S. *Brownian motion and stochastic calculus* (Graduate texts in mathematics). New York: World Publishing Company, 1988.
39. Deng H, Krstic M and Williams RJ. Stabilization of stochastic nonlinear systems driven by noise of unknown covariance. *IEEE T Automat Contr* 2001; 46(8): 1237–1253.
40. Loria A and Nijmeijer H. Bounded output feedback tracking control of fully actuated Euler–Lagrange systems. *Syst Control Lett* 1998; 33(3): 151–161.